NUMERICAL INVESTIGATION OF PRANDTL NUMBER EFFECTS ON THE NATURAL CONVECTION HEAT TRANSFER FROM CIRCULAR CYLINDER IN AN ENCLOSED ENCLOSURE

Omar **M**ohammed **A**li
Department of Refrigeration and Air Conditioning, Technical Institute of Zakho, Kurdistan - Region, Iraq.
(Accepted for publication: August 12, 2014)

ABSTRACT

In the present work, the natural convection heat transfer from horizontal circular cylinder situated in a square enclosure is investigated numerically. The work investigates the effect of Prandtl numbers on the flow and heat transfer characteristics. The study uses different Prandtl numbers (0.03, 0.7, 7, and 50), different Raylieh numbers (10^4, 10^5, and 10^6) and different enclosure width to cylinder diameter ratios W/D (1.667, 2.5 and 5). The work included the solution of the governing equations in the vorticity-stream function formulation which were transformed into body fitted coordinate system. The transformations are based initially on algebraic grid generation and elliptic grid generation to map the physical domain between the heated horizontal cylinder and the enclosure into a computational domain. The disecritization equation system are solved by using finite difference method. The code build using Fortran 90 to execute the numerical algorithm.

The results were compared with previous numerical results, which showed good agreement. The effect of Prandtl number variation on the average Nusselt numbers, flow patterns and isotherms with different Raylieh numbers and enclosure width ratios were investigated. The flow patterns and temperature distributions are presented by means of streamlines and isotherms, respectively. The results show that the streamlines and isotherms for Pr=0.03 are unique and differ from those of other higher Prandtl numbers for all enclosure widths and $Ra \geq 10^5$. The streamlines and isotherms for Pr≥0.7 are nearly similar and independent of Prandtl number. The same behaviors as streamlines and isotherms occur with Nusselt number for lower and higher values of Prandtl numbers with all ratios of enclosure width to cylinder diameter.

KEYWORDS: *Heat Transfer, Circular Cylinder, Square Enclosure, Numerical.*

NOMENCLATURE

Symbol	Definition	Unit
Nu	Average Nusselt number, (h.D/k).	
D	Cylinder diameter.	m
$d_{i,j}$	Source term in the general equation, eqn. (12).	
H	Convective heat transfer coefficient.	$W/m^2.°C$
J	Jacobian.	
K	Thermal conductivity of the air.	W/m.°C
P	Pressure.	N/m^2
P	Coordinate control function.	
Pr	Prandtl number, (ν/α).	
Q	Coordinate control function.	
R	maximum absolute residual value.	
Ra	Raylieh number, ($g\beta\Delta TD^3/\nu\alpha$).	
T	Time.	seconds
T	Temperature.	°C
U	Velocity in x-direction.	m/s
V	Velocity in y-direction.	m/s
W	Enclosure Width.	cm
W	Relaxation factor.	
X	Horizontal direction in physical domain.	m
X	Dimensionless horizontal direction in physical domain.	
y	Vertical direction in physical domain.	m
Y	Dimensionless vertical direction in physical domain.	
	Greek Symbols	
ΔT	Difference between cylinder surface temperature and environmental temperature.	°C
μ	Viscosity of the air.	kg/m.s

β	Coefficient of thermal expansion.	1/°C
η	Vertical direction in computational domain.	
ξ	Horizontal direction in computational domain.	
Ψ	Dimensionless stream function.	
ω	Vorticity.	1/s
ϖ	Dimensionless vorticity.	
υ	Kinematic viscosity.	m^2/s
α	Thermal diffusivity.	m^2/s
θ	Dimensionless temperature.	
ϕ	Dependent variable.	
ψ	Stream Function.	1/sec.
	Subscript	
S	Cylinder surface.	
∞	Environment.	
X	Derivative in x-direction.	
Y	Derivative in y-direction.	
ξ	Derivative in ξ-direction.	
D	Circular cylinder diameter.	
ψ	Stream function.	
T	Temperature.	
ω	Vorticity	

INTRODUCTION

The flow and thermal fields in enclosed space are of great importance due to their wide applications such as in solar collector-receivers, cooling of electronic equipment, aircraft cabin insulation, thermal storage system, and cooling systems in nuclear reactors, etc. A large number of literatures were published in the past decades. The effects of Prandtl number on natural convection heat transfer are of great interest. The Prandtl number is defined as the ratio of the kinematic viscosity of a fluid to its thermal diffusivity, $= \frac{\nu}{\alpha}$, which could vary over several orders of magnitude from 10^{-2} to 10^5 for common fluids. For example, the family of liquid metals has a small Prandtl number ($Pr<10^{-1}$) and on the contrary, the Prandtl number of engine oils is extremely large ($Pr>10^2$). Moreover, air and many other gases, water, and the family of hydrocarbons occupy the intermediate range ($10^{-1}<Pr<10^2$) of the entire spectrum. Since the Prandtl number serves as a measure of the viscous diffusion rate relative to the thermal diffusion rate, fluids with different Prandtl numbers could have quite different natural convective flow and heat transfer characteristics in enclosures or confined layers, Zi-Tao Yu et al., 2010.

Natural convective heat transfer in horizontal annuli between two concentric circular cylinders has been well studied. A comprehensive review was presented by Kuehn and Goldstein, 1976. Comparatively, little work has been done on natural convective heat transfer in more complex annuli such as the problem considered in this study. A few publications were involved in the experimental study. Ekundayo et al., 1998, studied natural convection in horizontal annulus between an outer square cylinder and an inner circular cylinder. In their study, a cylindrical heater with diameter of 9.5 mm was placed at different locations within a 350 mm×350 mm square-sectioned cold enclosure. The aspect ratio, i.e., the side length of the outer square cylinder over the diameter of the inner cylinder, is 36.84, which is large. It was found that the maximum steady-state rate of natural convection occurred when the heater was located parallel to and near a vertical wall. A few publications were also found for numerical investigations. Moukalled and Acharya, 1996, studied numerically natural convective heat transfer from a heated horizontal cylinder placed concentrically inside a square enclosure. The governing equations in their work are solved in a body-fitted coordinate system using a control volume-based numerical procedure. Shu et. al., 2002, studied the natural convection in a concentric annulus between a cold outer square cylinder and a heated inner circular cylinder is simulated using the differential quadrature (DQ)method. The authors found that both the aspect ratio and the Rayleigh number are critical to the patterns of flow and thermal fields. They suggests that a critical aspect ratio may exist at high Rayleigh number to distinguish the flow and thermal patterns. However, although there are a great many papers that have documented the Prandtl number effects on natural convection in enclosures. Koca et al., 2007, numerically investigated the Prandtl number effect on natural convection in a horizontal triangular enclosure that is locally heated on the bottom. Zi-Tao Yu et al., 2010, studied parametrically the effects of Prandtl number on laminar natural convection heat transfer in a horizontal equilateral triangular

cylinder with a coaxial circular cylinder is conducted. The Prandtl number is varied over a wide range from 10^{-2} to 10^{5}, which corresponds to a variety of working fluids. The governing equations with the Boussinesq approximation for buoyancy are iteratively solved using the finite volume approach. It is shown that the flow patterns and temperature distributions are unique for low-Prandtl number fluids (Pr≤0.1), and are nearly independent of Prandtl number when Pr≥0.7. In addition, the inclination angle of the triangular enclosure is found to noticeably affect the variations of the local Nusselt number, and to have insignificant influence on the average Nusselt numbers for low Rayleigh numbers when Pr≥0.7.

The present work deals with numerical investigation of natural convection heat transfer from circular horizontal cylinder situated in an enclosed square enclosure. The effect of Prandtl numbers with different Raylieh numbers Ra, and enclosure width on the Nusselt number will be investigated. The behaviors of the flow and temperature distribution will also be investigated to gain insight in the effect of studied variables on the flow hydrodynamics and thermal behavior.

MATHEMATICAL FORMLATION

The governing equations of the flow between the heated horizontal cylinder and the enclosure, that shown in figure (1), were based on the assumptions that the flow is Boussinesq, incompressible, no internal heat sources, laminar flow, and two-dimensional, Ali, 2008.

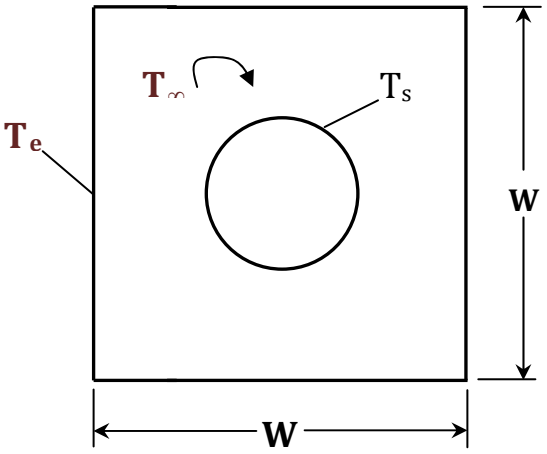

Figure (1): Configuration of cylinder-enclosure combination

The governing equations include the equation of continuity, momentum and the energy equation, Bejan and Kraus, 2003. These equations are presented below:

$$\frac{\partial u}{\partial x}+\frac{\partial v}{\partial y}=0 \qquad (1)$$

The x –momentum equation is:

$$\frac{\partial u}{\partial t}+u\frac{\partial u}{\partial x}+v\frac{\partial u}{\partial y}=-\frac{1}{\rho}\frac{\partial p}{\partial x}+\frac{\partial}{\partial x}\left(\mu\frac{\partial u}{\partial x}\right)+\frac{\partial}{\partial y}\left(\mu\frac{\partial u}{\partial y}\right)+g\beta\Delta T \qquad (2)$$

The y –momentum equation is:

$$\frac{\partial v}{\partial t}+u\frac{\partial v}{\partial x}+v\frac{\partial v}{\partial y}=-\frac{1}{\rho}\frac{\partial p}{\partial y}+\frac{\partial}{\partial x}\left(\mu\frac{\partial v}{\partial x}\right)+\frac{\partial}{\partial y}\left(\mu\frac{\partial v}{\partial y}\right) \qquad (3)$$

The energy equation is:

$$\rho c\left(\frac{\partial T}{\partial t}+u\frac{\partial T}{\partial x}+v\frac{\partial T}{\partial y}\right)=\frac{\partial}{\partial x}\left(k\frac{\partial T}{\partial x}\right)+\frac{\partial}{\partial y}\left(k\frac{\partial T}{\partial y}\right) \qquad (4)$$

Where μ is the laminar viscosity.

With Boussinesq approximations, the density is constant for all terms in the governing equations except for the buoyancy force term that the density is a linear function of the temperature.

$$\rho = \rho_o(1-\beta\Delta T) \tag{5}$$

Where β is the coefficient of thermal expansion.

The stream function (ψ) and vorticity (ω) in the governing equations are defined as follows, Anderson, 1995 and Petrovic, 1996:

$$u = \frac{\partial\psi}{\partial y}, \quad v = -\frac{\partial\psi}{\partial x} \tag{6}$$

$$\omega = \frac{\partial v}{\partial x} - \frac{\partial u}{\partial y} \tag{7}$$

Or $\omega = \nabla \times \vec{V}$

the governing equations for laminar flow become:

Energy Equation:

$$\frac{\partial\theta}{\partial t} + \frac{\partial\Psi}{\partial y}\frac{\partial\theta}{\partial x} - \frac{\partial\Psi}{\partial x}\frac{\partial\theta}{\partial y} = \left(\frac{\partial^2\theta}{\partial x^2} + \frac{\partial^2\theta}{\partial y^2}\right) \tag{8}$$

Momentum Equation:

$$\frac{\partial\varpi}{\partial t} + \frac{\partial\Psi}{\partial y}\frac{\partial\varpi}{\partial x} - \frac{\partial\Psi}{\partial x}\frac{\partial\varpi}{\partial y} = \Pr\left(\frac{\partial^2\varpi}{\partial x^2} + \frac{\partial^2\varpi}{\partial y^2}\right) + Ra\Pr\frac{\partial\theta}{\partial x} \tag{9}$$

Continuity Equation:

$$\frac{\partial^2\Psi}{\partial x^2} + \frac{\partial^2\Psi}{\partial y^2} = -\varpi \tag{10}$$

In the stream function-vorticity formulation, there is a reduction in the number of equations to be solved in the ψ-ω formulation, and the troublesome pressure terms are eliminated in the ψ-ω approach.

The dimensionless variables in the above equations are defined as:

$$X = \frac{x}{D}, \quad Y = \frac{y}{D}, \quad U = \frac{uD}{\vartheta}, \quad V = \frac{vD}{\vartheta},$$

$$\tau = \frac{t\vartheta}{D^2}, \quad \Psi = \frac{\psi}{\vartheta}, \quad \varpi = \frac{\omega D^2}{\vartheta}, \quad \theta = \frac{T - T_\infty}{T_c - T_\infty} \tag{11}$$

The cylinder diameter D is the characteristic length in the problem. By using the above parameters,

The governing equations (8)-(10) transformed to the following general form in the computational space:

$$a_\phi\left\{\frac{\partial\phi}{\partial t} + \frac{1}{J}\left[\left(\frac{\partial\psi}{\partial\eta}\phi\right)_\xi - \left(\frac{\partial\psi}{\partial\xi}\phi\right)_\eta\right]\right\} = \nabla\left(b_\phi\nabla\phi\right) + d_\phi \tag{12}$$

Where ϕ is any dependent variable.

The governing equations represented by interchanging the dependent variable ϕ for three governing equations as follow

ϕ	a_ϕ	b_ϕ	d_ϕ
ψ	0	1	ω
ω	1	μ	$\frac{g\beta}{J}\left[\left(y_\eta\theta\right)_\xi - \left(y_\xi\theta\right)_\eta\right]$
T	1	μ/k	0

$\frac{\partial\phi}{\partial t}$ represents the unsteady term.

$\frac{1}{J}\left[\left(\frac{\partial\psi}{\partial\eta}\phi\right)_\xi - \left(\frac{\partial\psi}{\partial\xi}\phi\right)_\eta\right]$ is the convective term.

$\nabla\left(b_\phi\nabla\phi\right)$ is the diffusion term.

In addition, d_ϕ is the source term.

Grid Generation

The algebraic grid generation method is used to generate an initial computational grid points. The elliptic partial differential equations that used are Poisson equations:

$$\xi_{xx} + \xi_{yy} = P(\xi,\eta) \tag{13a}$$

$$\eta_{xx} + \eta_{yy} = Q(\xi,\eta) \tag{13b}$$

Interchanging dependent and independent variables for equations (13a, and b), gives:

$$\alpha x_{\xi\xi} - 2\beta x_{\xi\eta} + \gamma x_{\eta\eta} + J^2\left(P x_\xi + Q x_\eta\right) = 0 \tag{14a}$$

$$\alpha y_{\xi\xi} - 2\beta y_{\xi\eta} + \gamma y_{\eta\eta} + J^2\left(P y_\xi + Q y_\eta\right) = 0 \tag{14b}$$

Where $\alpha = x_\eta^2 + y_\eta^2$; $\beta = x_\xi x_\eta + y_\xi y_\eta$;

$\gamma = x_\xi^2 + y_\xi^2$

The coordinate control functions P and Q may be chosen to influence the structure of the grid, Thomas et. al., 1980. The solution of Poisson equation and Laplace equation are obtained using Successive over Relaxation (SOR) method with relaxation factor value equal to 1.4, Hoffman, 1989 and Thompson, 1985.

The transformation of the physical domain into computational domain using elliptic grid generation is shown in figure (2).

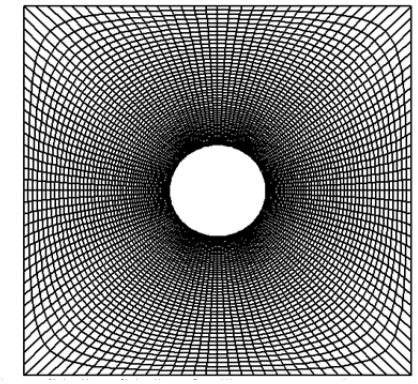

Figure (2) Transformations of the physical domains into computational domains using elliptic grid generation.

Method Of Solution

In the present study, the conversion of the governing integro-differential equations into algebraic equations, amenable to solution by a digital computer, is achieved by the use of a Finite Volume based Finite Difference method, Ferziger, 2002.

To avoid the instability of the central differencing scheme (second order for convective term) at high Peclet number (Cell Reynolds Number) and an inaccuracy of the upwind differencing scheme (first order for convective term) the hybrid scheme is used. The method is hybrid of the central differencing scheme and the upwind differencing scheme.

$$a_P \phi_P = a_E \phi_E + a_W \phi_W + a_N \phi_N + a_S \phi_S + a_P^o \phi_P^o + a_M \left(\phi_{i+1,j+1} - \phi_{i-1,j-1} - \phi_{i+1,j-1} + \phi_{i-1,j+1}\right) + d_{i,j} \quad (15)$$

$$a_P = a_E + a_W + a_N + a_S + a_P^o \quad (16)$$

The resulting algebraic equation is solved using alternating direction method ADI in two sweeps; the first sweep, the equations are solved implicitly in ξ-direction and explicitly in η-direction. The second sweep, the equations are solved implicitly in η-direction and explicit in ξ-direction. In first sweep, the implicit discretization equation in ξ-direction is solved by using Cyclic TriDiagonal Matrix Algorithm (CTDMA) because of its cyclic boundary conditions. In second sweep, the implicit discretization equation in η-direction is solved by using TriDiagonal Matrix Algorithm (TDMA).

The solution of the stream function equation was obtained using Successive Over-Relaxation method (SOR).

The initial conditions of the flow between heated cylinder and vented enclosure are:

$\Psi=0,\ \theta = 0,\ \omega = 0$ For $t = 0$ (17)

The temperature boundary condition of the cylinder surface assumed as constant.

$$\left.\frac{\partial\theta}{\partial\eta}\right|_m = 0 \quad \text{at enclosure wall} \quad (18a)$$

Using 2nd order difference equation, the temperature at the enclosure surface becomes:

$$\theta_{i,m} = \frac{4}{3}\theta_{i,m-1} - \frac{1}{3}\theta_{i,m-2} \quad (18b)$$

Vorticity boundary conditions, Roache, 1982, are

$$\varpi = \frac{2\gamma}{J^2}\left(\psi_{i,m} - \psi_{i,m-1}\right) \quad \text{at enclosure wall} \quad (19a)$$

$$\varpi = \frac{2\gamma}{J^2}\left(\psi_{i,1} - \psi_{i,2}\right) \quad \text{at cylinder surface} \quad (19b)$$

The stream function of the cylinder is assumed as zero because the cylinder is a continuous solid surface and no matter enters into it or leaves from it. The stream function of the enclosure is assumed as constant.

The Nu is a nondimensional heat transfer coefficient that calculated in the following manner:

$$Nu = \frac{\sqrt{\gamma}}{J}\int_0^{2\pi}\frac{\partial\theta}{\partial\eta}d\zeta \qquad (20a)$$

The derivative of the nondimensional temperature is calculated using the following formula, Fletcher, 1988 :

$$\left.\frac{\partial\theta}{\partial n}\right|_{\eta=const.} = \frac{1}{J\sqrt{\gamma}}\left(-\beta\theta_\xi + \gamma\theta_\eta\right) = \frac{\sqrt{\gamma}}{J}\frac{\partial\theta}{\partial\eta} \qquad (20b)$$

$\theta_\xi = 0$ at cylinder surface

A computer program in (Fortran 90) was built to execute the numerical algorithm which is mentioned above; it is general for a natural convection from heated cylinder situated in an enclosure.

RESULTS AND DISCUSSION

In the present study, different fluids were used as the working fluids and the Prandtl number ranged between (0.03-50). The numerical work deals with natural convection heat transfer from circular horizontal cylinder when housed in an enclosed square enclosure. The cases for three different aspect ratios W/D =5, 2.5 and 1.67 and Rayleigh numbers of 10^4, 10^5, and 10^6 were studied.

After numerical discretization by the Hybrid method, the resultant algebraic equations are solved by the ADI method. The convergence criteria are chosen as $R_T<10^{-6}$, $R_\psi<10^{-6}$ and $R_\omega<10^{-6}$ for T, ψ and ω respectively. When all the three criteria are satisfied, the convergent results are subsequently obtained.

Stability And Grid Independency Study

The stability of the numerical method is investigated for the case Ra=10^5, W/D=2.5, Pr = 0.7. Three time steps are chosen with values 1×10^{-4}, 5×10^{-4}, 5×10^{-6}. The maximum difference between the values of Nu with different time steps is 2%. The numerical method becomes unstable with time step 10^{-4} at Pr ≠0.7, therefore; the time step of the method decreases with changing the value of the Prandtl number.

The grid-independence of numerical results is studied for the case with Ra=10^4, and 10^5, W/D =2.5, Pr = 0.7. The three mesh sizes of 96×25, 128×45, and 192×50 are used to do grid-independence study. It is noted that the total number of grid points for the above three mesh sizes is 2425, 5805, and 9650 respectively. Numerical experiments showed that when the mesh size is above 96×45, the computed Nu remain the same. The same accuracy is not obtainable with W/D=5 and high Raylieh numbers, therefore; the mesh size 128×45 is used in the present study for all cases.

Validation Test

The code build using Fortran 90 to execute the numerical algorithm. To test the code validation, the natural convection problem for a low temperature outer square enclosure and high temperature inner circular cylinder was tested. The calculations of average Nusselt numbers and maximum stream function ψ_{max} for the test case are compared with the benchmarks values by Moukalled and Acharya, 1996, for different values of the enclosure width to cylinder diameter ratios (W/D=1.667, 2.5, and 5) with Rayleigh numbers Ra=10^4 and 10^5 as given in table (1). From table 1, it can be seen that the present results generally agree well with those of Moukalled and Acharya, 1996.

Table (1): Comparisons of Nusselt numbers and maximum stream function with Previous data.

L/D	Ra	ψ_{max}		$\overline{Nu}$	
		Present	Moukalled and Acharya, 1996	Present	Moukalled and Acharya, 1996
5.0	10^4	2.45	2.08	1.7427	1.71
2.5		3.182	3.24	0.9584	0.97
1.67		5.22	5.4	0.4274	0.49
5.0	10^5	10.10	10.15	3.889	3.825
2.5		8.176	8.38	4.93	5.08
1.67		4.8644	5.10	6.23	6.212

Flow Patterns and Isotherms For W/D=1.667

Flow Patterns

The numerical solutions for four Prandtl numbers were obtained. The Prandtl number values are: Pr = 0.03, 0.7, 7, and 50 will be presented herein. At W/D = 1.677, the Prandtl number effects on natural convection flow patterns, demonstrated by streamlines, are shown in Fig. (3). The circular cylinder diameter is relatively large and the physical domain between the circular cylinder and the enclosure is small. The maximum stream function value varies between Ψmax=0.48 at Ra=104 to Ψmax=8.8 at Ra=106 for low Prandtl number (Pr=0.03), while; it varies between Ψmax=0.464 at $Ra=10^4$ to Ψmax =22.1 at $Ra=10^6$ for higher Prandtl numbers ($Pr\geq0.7$). The maximum stream function value for Pr=0.03 decreases because the convective flow is dominated by the inertia flow rather than viscous flow. The flow is symmetrical about the vertical line through the center of the circular cylinder for all cases. The flow patterns for Pr = 0.03, $Ra\geq10^5$ are unique and completely different from those for higher Prandtl numbers $Pr\geq0.7$. At $Ra=10^4$, the flow circulation is very weak and the maximum stream function value is small. The streamlines for all Prandtl numbers are similar and independent of Prandtl numbers with little difference in the streamlines for Pr=0.03. The flow patterns appear as a curved kidney-shaped dual-kernel eddy. At $Ra=10^5$, the flow circulation becomes stronger than $Ra=10^4$ and the stream function value increases. The flow patterns for Pr=0.03 are unique and completely different from those of higher Prandtl numbers. Multiple eddies appear for Pr=0.03, while; appear two tiny eddies near the vertical center line in addition to the eddies around the cylinder for higher Prandtl numbers $Pr\geq0.7$. The flow patterns of Pr=0.03 becomes slightly oscillatory in the lower part of the annulus and the steady-state solution is not available because the convective flow is dominated by the inertia force rather than the viscous force. The flow appear as four eddies, two of them are nearly circular-shaped near the upper corners of the enclosure, and other two eddies appear as nearly elliptical-shaped. It is noted the appearance of two tiny eddies near the vertical center line. The nearly circular-shaped eddies have little densely packed. For $Pr\geq0.7$, the flow patterns are similar and independent of Prandtl number. At $Ra=10^6$, the maximum stream function values increase for all Prandtl numbers. The flow circulation become stronger than other Raylieh numbers. The number of eddies increases to six eddies, four of them near the corners of the enclosure and two eddies inside the tiny eddies. The eddies become more densely packed. The flow patterns for Pr=0.7 differ from those of other higher Prandtl numbers. The eddies move upward and the stagnant area become more. A single large kernel eddy appears for Pr=0.7 rather than the small dual kernel eddies for $Pr\geq7$. The flow patterns cover most of the physical space between the cylinder and the enclosure and the area is very small.

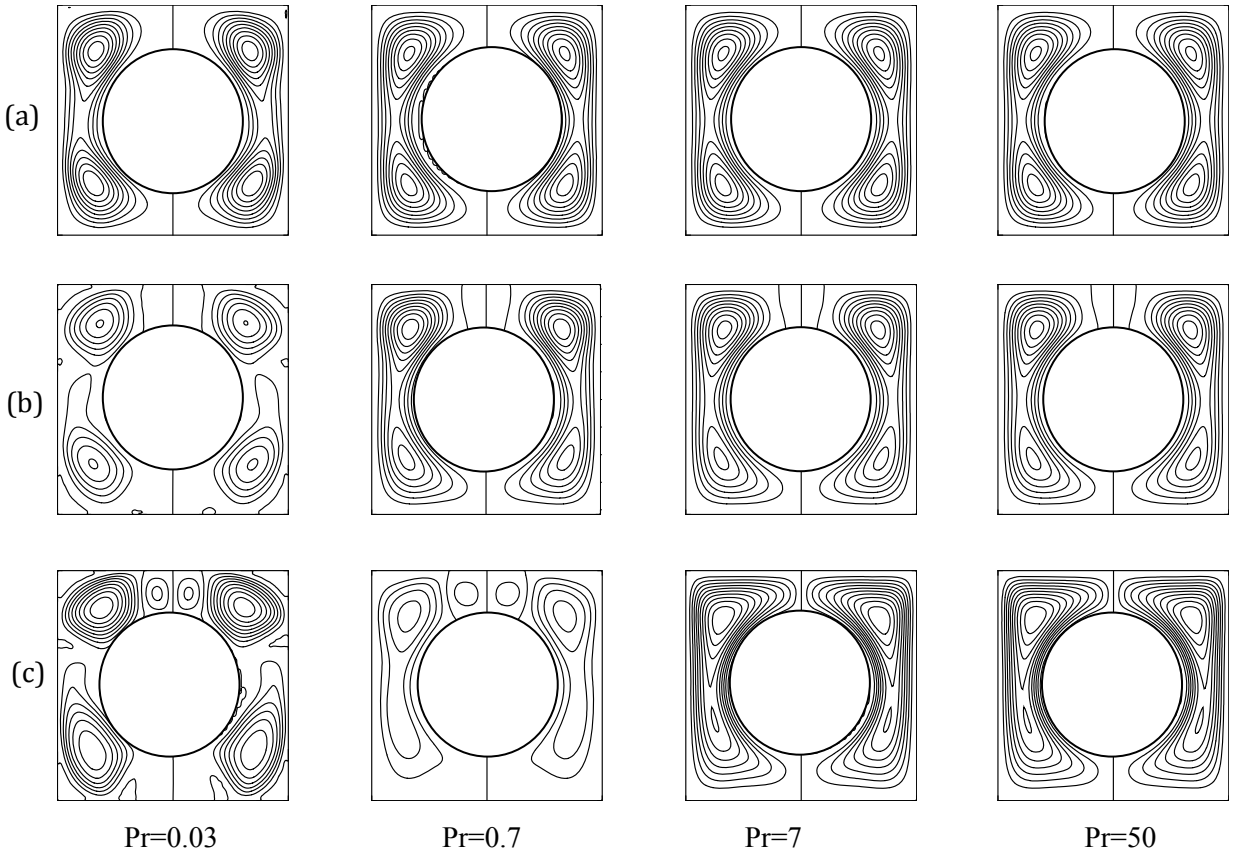

Figure (3) Effect of Prandtl number on streamlines at W/D = 1.67 and (a) Ra = 10^4, (b) Ra = 10^5, (c) Ra = 10^6.

Temperature Fields:

The characteristics of the temperature distributions are presented by means of isotherms in figure (4). The same arrangements as flow patterns are displayed in the figure with same Prandtl numbers and Raylieh numbers. The isotherms are symmetrical about the vertical line through the center of the circular cylinder.

At Ra=10^4, the isotherms are similar and independent of Prandtl number for all Prandtl numbers. The isotherms display as rings around the cylinder. The shape of the isotherms ensure that the mode of heat transfer is pure conduction and the effect of the convection is very low. At Ra=10^5, the temperature distributions for higher Prandtl numbers are similar and independent of Prandtl number. They have small distortions below the cylinder due to the effect of the convection heat transfer. The isotherms for Pr=0.03 are unique and differ from other Prandtl numbers. The distortion of the isotherms become more around the cylinder due to the effect of the convection heat transfer. At Ra=10^6, the effect of natural convection on the heat transfer increases. For Pr≥7, a thermal plume impinging to the top of the enclosure. Pair of thermal plumes appear on the top of the cylinder with about 45° from the vertical center line. For Pr=0.7, a thermal plume with reverse direction appears on the top of the cylinder, in addition to two thermal plumes display with about 30° from the vertical center line. A thermal stratification (horizontal and flat isotherms) are formed for Pr≥0.7. The isotherms become more flat in the middle region below the cylinder for Pr≥7.

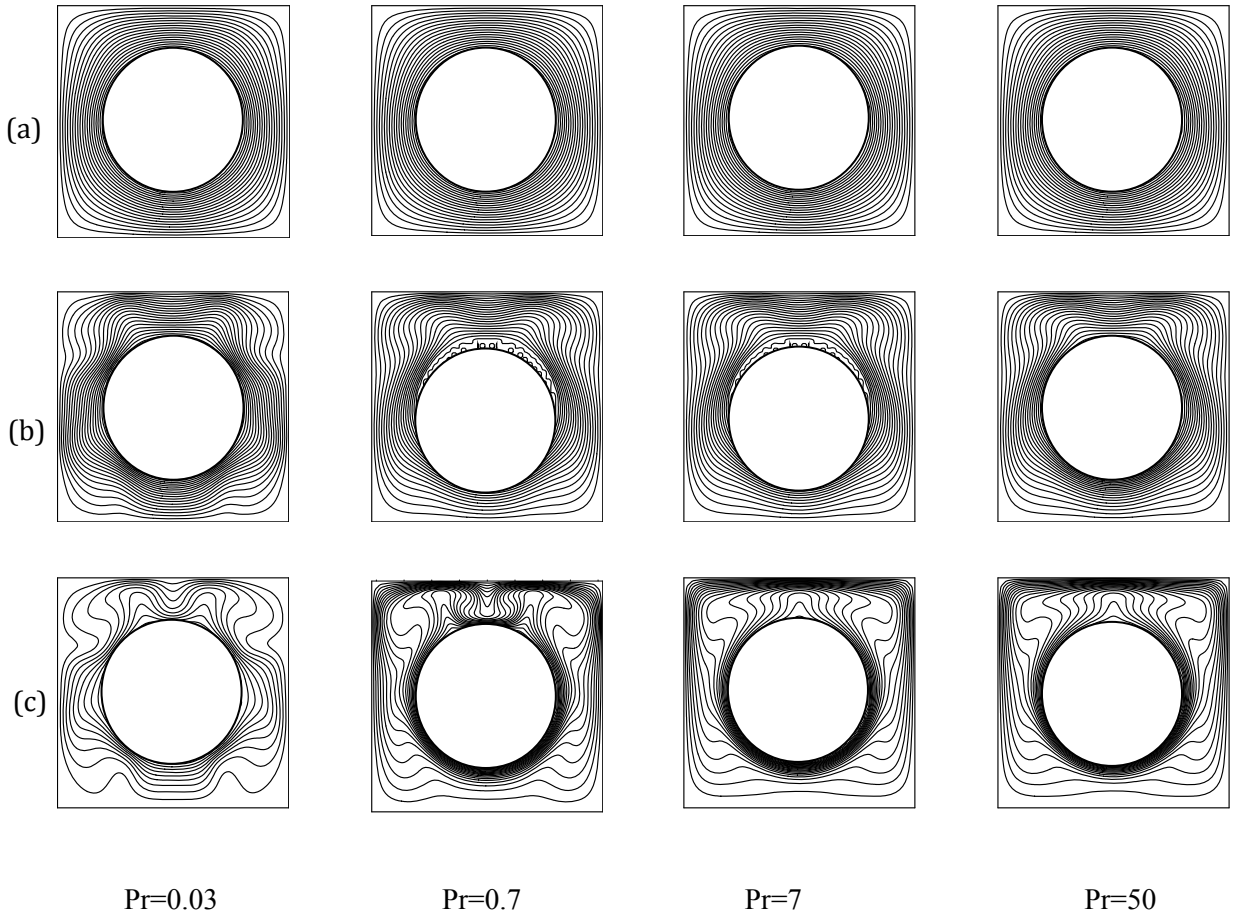

Figure (4) Effect of Prandtl number on isotherms at W/D = 1.67 and (a) Ra = 10^4, (b) Ra = 10^5, (c) Ra = 10^6.

Flow Patterns and Isotherms For W/D=2.5

Flow Patterns

The flow patterns for Prandtl number Pr = 0.03, 0.7, 7, and 50 with Raylieh numbers Ra=10^4, 10^5, 10^6 are presented in figure(5). The same arrangements that uses for the streamlines of the case W/D = 1.677 are presented herein. At W/D=2.5, the Prandtl number effects on natural convection flow patterns are demonstrated by streamlines, as shown in Fig.(5). The circular cylinder diameter reduces and the physical domain between the circular cylinder and the enclosure enlarges. The maximum stream function value varies between Ψ_{max}=0.87 at Ra=10^4 to Ψ_{max}=12.73 at Ra=10^6 for low Prandtl number (Pr=0.03), while; it varies between Ψ_{max}=1.739 at Ra=10^4 to Ψ_{max}=24.78 at Ra=10^6 for higher Prandtl numbers (Pr≥0.7). As the case W/D=1.67, the maximum stream function value for Pr=0.03 decreases because the convective flow is dominated by the inertia flow rather than viscous flow. For all Prandtl numbers and Raylieh numbers, the flow is symmetrical about the vertical line through the center of the circular cylinder. The flow patterns for Pr= 0.03 and all Raylieh numbers are unique and completely different from those for higher Prandtl numbers Pr≥0.7. At Ra=10^4, the flow circulation is weak, it become stronger than the flow circulation for W/D=1.67. The maximum stream function value is small. The streamlines for higher Prandtl numbers Pr≥0.7 are similar and independent of Prandtl numbers. The flow patterns appear as a curved kidney-shaped contain dual kernel eddies with different sizes. The flow patterns for Pr=0.03 are differ from those of higher Prandtl numbers Pr≥0.7. The streamlines move to the sides and the stagnant area enlarges.

At Ra=10^5, the strength of the flow circulation becomes more, and the value of stream function increases. The flow patterns for higher Prandtl numbers Pr≥0.7 are nearly similar and independent of Prandtl number. A single

small kernel eddy appears rather than the dual kernel eddies for Ra=10^4 and Pr≥0.7. The size of kernel eddy for Pr=0.7 is larger than those for Pr≥7. The streamlines near the bottom enclosure wall move upward and the stagnant area becomes more. The flow patterns for Pr=0.03 are unique and completely different from those of higher Prandtl numbers. There exist four nearly circular-shaped eddies, which are slightly asymmetrical about y-axis through the cylinder. The flow becomes slightly oscillatory in the lower part of the annulus and the steady-state solution is not available because the convective flow is dominated by the inertia force rather than the viscous force. The eddies near the upper corners have more densely packed than those near the bottom corners. Two tiny eddies appear near vertical center line on the bottom enclosure wall. As Raylieh number increases to Ra=10^6, the flow becomes stronger and the maximum stream function increases for all Prandtl numbers. The flow are symmetrical about the vertical center line. The streamlines for Pr≥7 are similar and independent of the Prandtl number. The streamlines near the bottom enclosure wall move more and more to the upward that lead to an increase in the stagnant area. The streamlines near the upper enclosure wall are horizontal and flat. The size of the kernel becomes more. The flow patterns for Pr=0.7 are similar to those for Pr≥7, except the streamlines near the upper enclosure wall and upper corners appear as curvature. The appearance of multiple eddies continue for Pr=0.03 and Ra=10^6. The eddies become less densely packed, specially for lower eddies. Pair of tiny eddies appear near the vertical center line on the top of the cylinder.

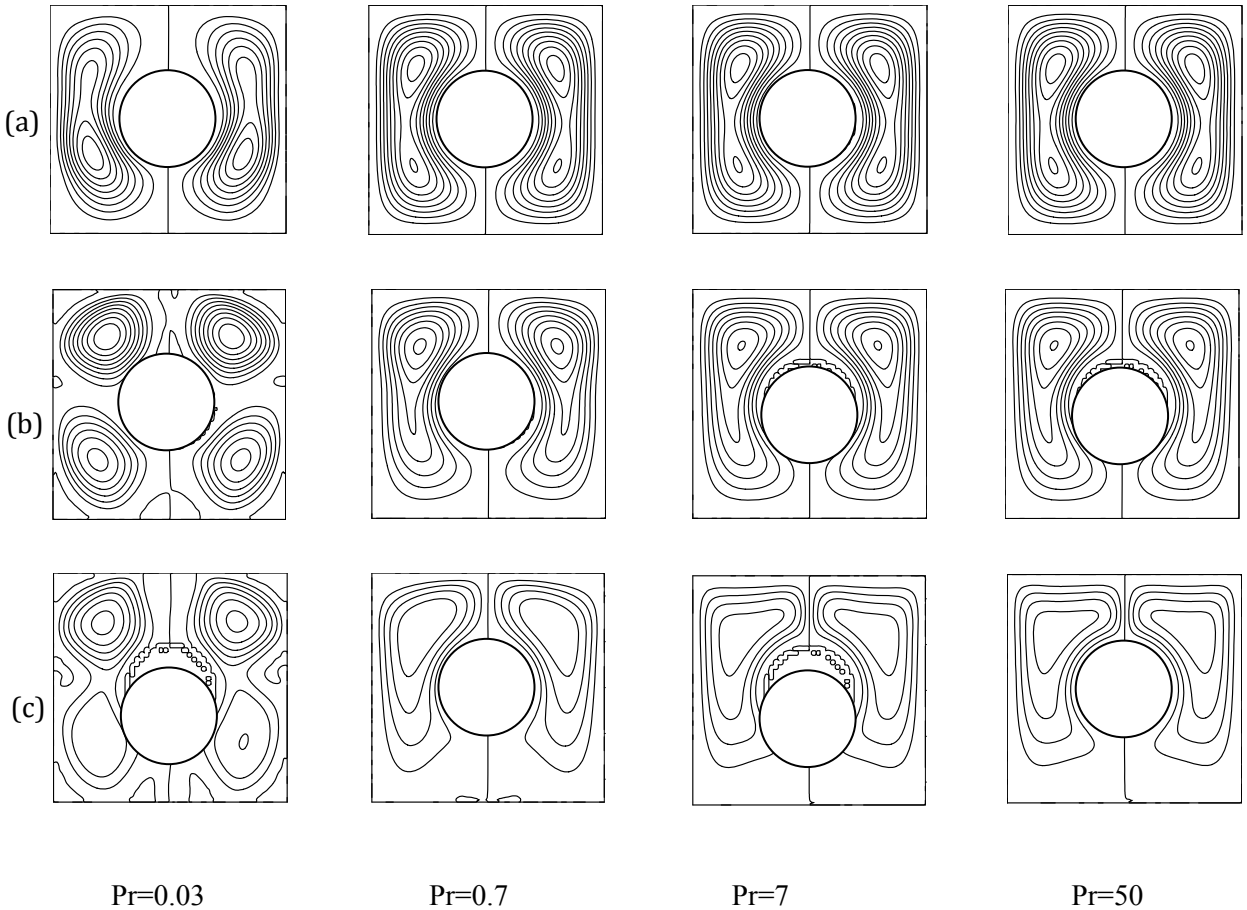

Figure (5) Effect of Prandtl number on streamlines at W/D = 2.5 and (a) Ra = 10^4, (b) Ra = 10^5, (c) Ra = 10^6.

Temperature Fields:

The temperature distributions for W/D=2.5 are presented by means of isotherms in figure (6). The same arrangements as flow patterns are displayed in the figure with same Prandtl numbers and Raylieh numbers. The isotherms are symmetrical about the vertical line through the center of the circular cylinder. As Raylieh number increases, the thermal boundary layer becomes thinner and thinner.

At $Ra=10^4$, the isotherms are similar and independent of Prandtl number for all Prandtl numbers. The mode of heat transfer is the conduction with very little effect of convection heat transfer. The isotherms display as circles around the cylinder. As Raylieh number increases to $Ra=10^5$, the temperature distributions are similar and independent of Prandtl number for $Pr\geq0.7$. The isotherms distorts below the cylinder due to the effect of the convection heat transfer. A thermal plume appear on the top of the cylinder. The isotherms for $Pr\geq7$ are horizontal and flat near the lower enclosure wall with very little distortion in the isotherms for Pr=0.7 at this region. The isotherms for Pr=0.03 are unique and differ from those of other Prandtl numbers. The distortion of the isotherms become more around the cylinder due to the effect of the convection heat transfer. At $Ra=10^6$, the convection becomes the dominant mode of heat transfer. The isotherms for $Pr\geq0.7$ are similar with slightly difference for Pr=0.7. A thermal plume impinging on the top of the enclosure. For $Pr\geq7$, the isotherms near the bottom enclosure wall become more flat and horizontal as compared with those for Pr=0.7. The thermal stratification (horizontal and flat isotherms) are formed at this region. Two thermal plumes displayed on the top of the cylinder with about 45° from the vertical center line. The curvature of the these plumes are less than those for Pr=0.7.

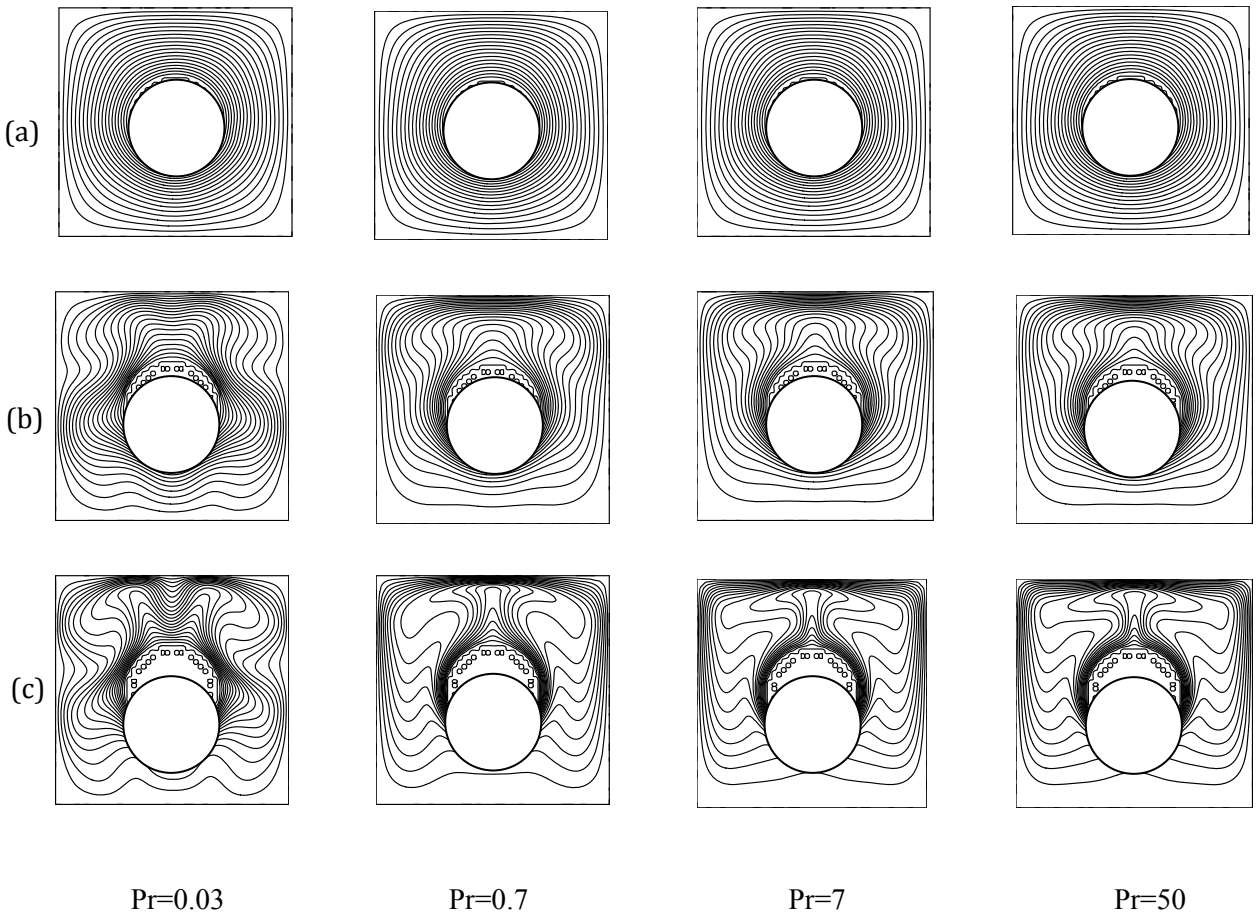

Figure (6) Effect of Prandtl number on isotherms at W/D = 2.5 and (a) $Ra = 10^4$, (b) $Ra = 10^5$, (c) $Ra = 10^6$.

Flow Patterns and Isotherms For W/D=5

Flow Patterns

The flow patterns for W/D=5 are presented herein by means of streamlines with Pr = 0.03, 0.7, 7, and 50 and Ra=10^4, 10^5, 10^6 as shown in figure (7). The same arrangements that use for the streamlines of the cases W/D = 1.677, and 2.5 are displayed herein. At W/D=5, the circular cylinder diameter is relatively small and the physical domain between the circular cylinder and the enclosure enlarges. The maximum stream function value varies between Ψ_{max}=1.215 at Ra=10^4 to Ψ_{max}=14.14 at Ra=10^6 for low Prandtl number (Pr=0.03), while; it varies between Ψ_{max}=1.81 at Ra=10^4 to Ψ_{max}=25.2 at Ra=10^6 for higher Prandtl numbers (Pr≥0.7). The maximum stream function value for Pr=0.03 decreases because the convective flow is dominated by the inertia flow rather than viscous flow. The flow patterns for Pr= 0.03 and all Raylieh numbers are unique and completely different from those for higher Prandtl numbers Pr≥0.7. At Ra=10^4, the flow circulation is weak, it become stronger than the flow circulation for previous cases. The streamlines for higher Prandtl numbers Pr≥0.7 are nearly similar and slightly independent of Prandtl numbers. The flow patterns appear as a curved kidney-shaped contain one kernel eddy for each side. The flow patterns for Pr=0.03 are differ from those of higher Prandtl numbers Pr≥0.7. The flow is asymmetrical about vertical line through circular cylinder. The flow circulation is weak. The stagnation area is large and the streamlines are less densely packed from those of other Prandtl numbers.

At Ra=10^5, the flow circulation becomes stronger, which, the value of maximum stream function increases. For Pr≥0.7, the streamlines are nearly similar and independent of Prandtl number, and the flow is symmetrical about vertical line through circular cylinder. The streamlines near the bottom of the enclosure wall move upward toward the cylinder and the stagnant area becomes more. The flow patterns for Pr=0.03 are unique and completely different from those for Pr≥0.7 for the same reason as mentioned in the previous cases W/D=1.67 and 2.5. The flow become slightly asymmetrical about y-axis through the cylinder. The shape of the streamlines seem as rings attached with a plume eddy below these circles. Multiple tiny eddies display near the enclosure walls. At Ra=10^6, the flow circulation becomes stronger and the maximum stream function increases for all Prandtl numbers. For Pr=0.03, the nearly circular-shaped eddies become more densely packed and the attached plumes direct to the sides of the enclosure. The number of tiny eddies around the enclosure increase. For Pr≥7, the streamlines near the bottom of the enclosure wall move upward to reach the bottom of the cylinder and the stagnant area becomes more and more. For Pr=0.7, the flow appear as nearly bean-shaped eddies, which are symmetrical, are formed. Two small eddies display near the center line at the lower enclosure wall.

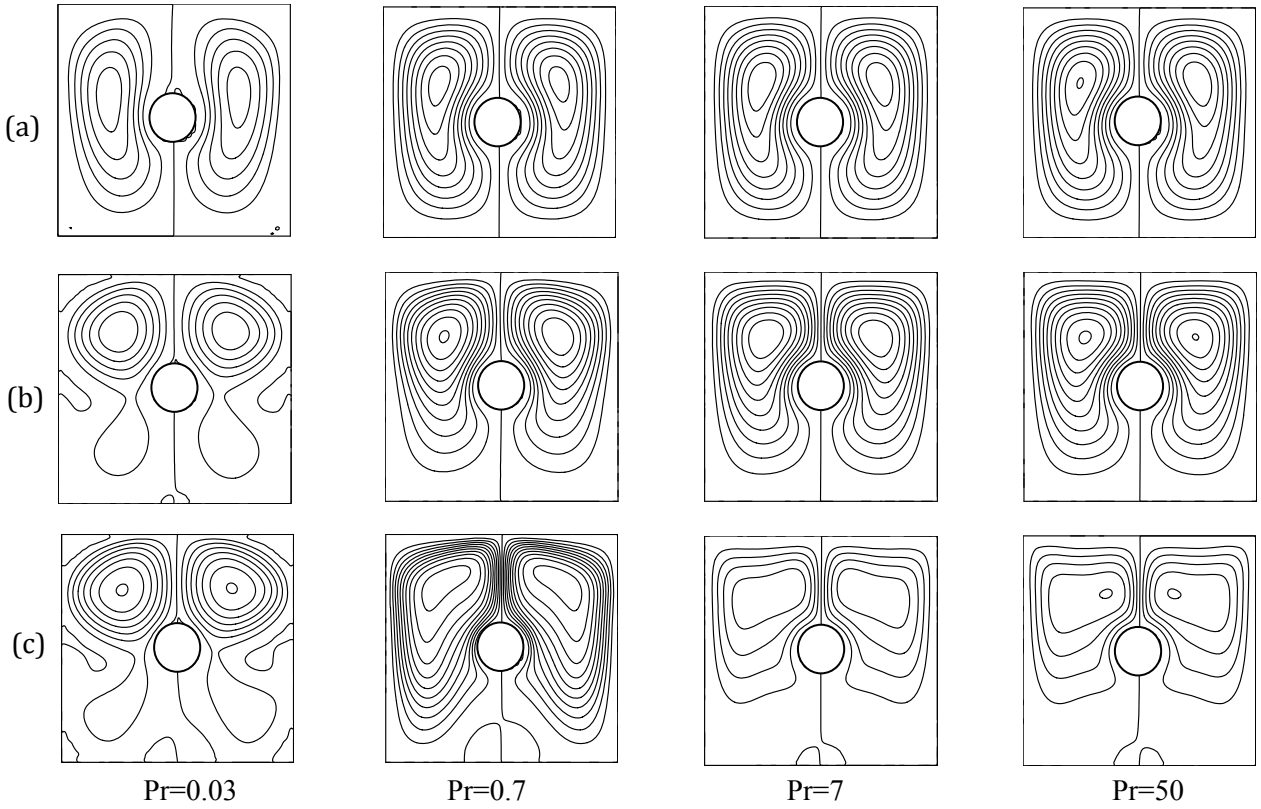

Figure (7) Effect of Prandtl number on streamlines at W/D = 5 and (a) Ra = 10^4, (b) Ra = 10^5, (c) Ra = 10^6.

Temperature Fields:

The temperature distributions for W/D=5 are presented by means of isotherms in figure (8). The same arrangements as flow patterns are displayed in the figure with same Prandtl numbers and Raylieh numbers. The isotherms are symmetrical about the y-axis line through the center of the circular cylinder. As Raylieh number increases, the thermal boundary layer becomes thinner and thinner.

At Ra=10^4, the isotherms are similar and independent of Prandtl number for all Prandtl numbers. The mode of heat transfer is the conduction with little contribution of convection heat transfer. The isotherms display as nearly elliptical-shaped around the cylinder. As Raylieh number increases to Ra=10^5, the isotherms distort below the cylinder for higher Prandtl numbers Pr≥0.7 due to the effect of the convection heat transfer. The temperature distributions appear as nearly similar and independent of Prandtl number. A thermal plume appear on the top of the cylinder. Two thermal plumes displayed on the top of the cylinder with about 60° from the y-axis center line. The isotherms for Pr=0.03 are unique and differ from those of other Prandtl numbers. The distortion of the isotherms become more around the cylinder due to the effect of the convection heat transfer. The thermal plume, which appears above top of the cylinder, is thicker than that for Pr≥0.7. Two thermal plumes are formed near the sides of the cylinder with reverse direction. At Ra=10^6, the convection becomes the dominant mode of the heat transfer. The isotherms for Pr≥0.7 are different. For Pr=0.7, a thinner thermal plume impinging on the top of the enclosure. Two plumes appear on top of the inner circular cylinder with about 60◦ from the vertical centre line. The isotherms below the cylinder are wavy. For Pr≥7, the thermal plume above top of the cylinder becomes thinner and increases its length. The isotherms below the cylinder become more flat and horizontal as compared with those for Pr=0.7. For Pr=0.03, the isotherms distort more and more, and appear as wavy around the cylinder. The thickness of the thermal plume above top of the cylinder is thicker from those for Pr≥0.7.

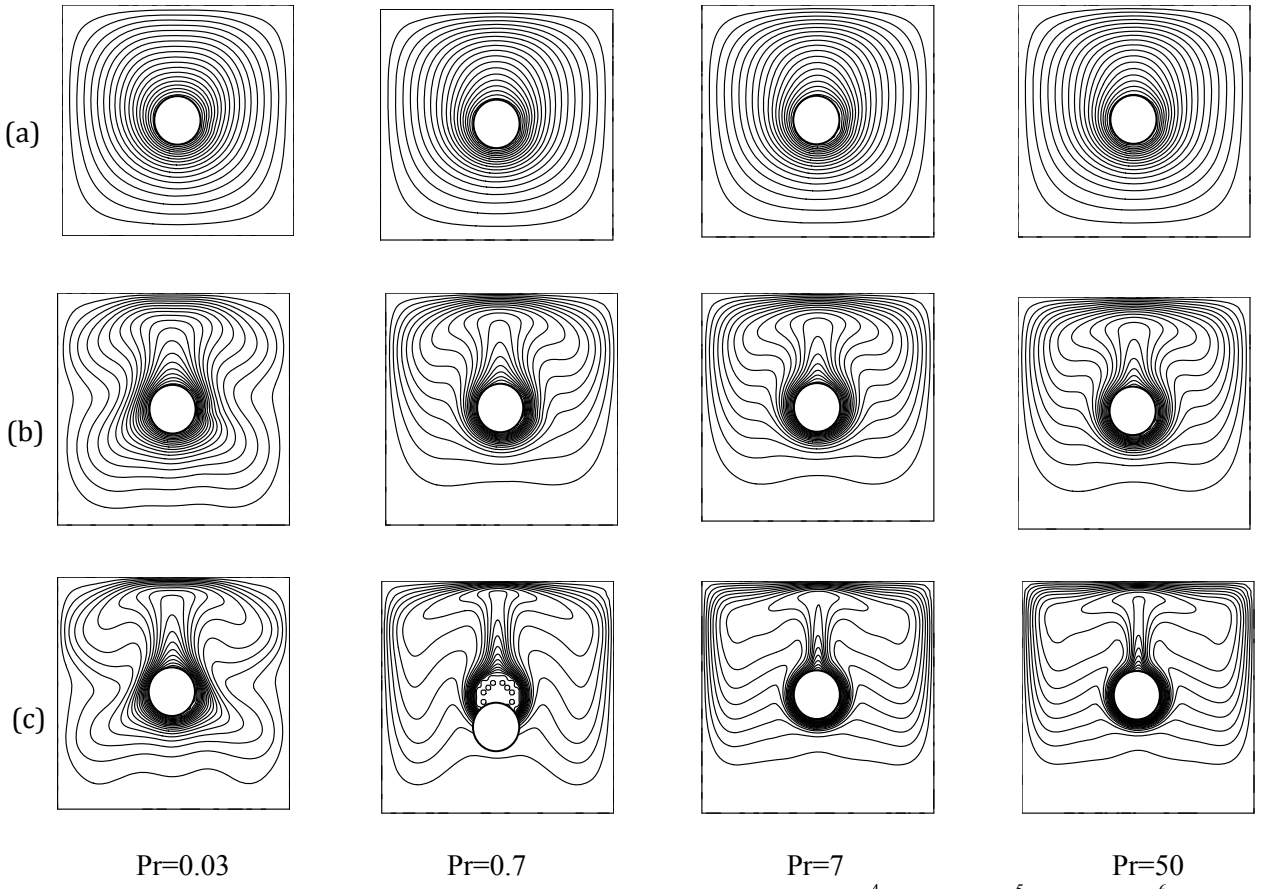

Figure (8) Effect of Prandtl number on isotherms at W/D = 5 and (a) Ra = 10^4, (b) Ra = 10^5, (c) Ra = 10^6.

Overall heat transfer and correlations

The average Nusselt number is chosen as the measure to investigate the heat transfer from the circular cylinder. The effect of Prandtl numbers on the average Nusselt numbers with Ra=10^4, 10^5, and 10^5 for enclosure width to the cylinder ratios W/D=1.67, 2.5 and 5 are presented in figures (9, 10, 11). The Prandtl numbers in the present study are:0.03, 0.7, 7, 50. The Nusselt number increases with increasing the Raylieh number for all Prandtl numbers and all enclosure width to cylinder diameter ratios W/D. At Ra=10^4, the Nusselt number do not change with the variation of the Prandtl number and the curves appear nearly flat because the conduction is the dominant mode of the heat transfer for all enclosure width to cylinder diameter ratios. At Ra=10^5, the relation between the Prandtl number and Nusselt number differ with the variation of the W/D. For W/D=1.67, figure (9), the Nusselt number independent of the Prandtl number, therefore; the curve is nearly horizontal and flat line. For W/D=2.5, figure (10), the Nusselt number slightly decreases for Pr=0.03, but the Nusselt number is independent of Prandtl number for Pr≥0.7, which means the relation between the Nusselt number and the Prandtl number is flat (constant value) for Pr≥0.7. The same behavior occurs for W/D=5, figure (11), the Nusselt number is independent of Prandtl number and slightly constant for Pr≥0.7. The Nusselt number of Pr=0.03 is lower than that for Pr≥0.7 by 1. At Ra=10^6 and W/D=1.67, figure (9), the maximum Nusselt number value obtains at Pr=0.7, and decreases as Prandtl number increases to Pr=7 and remains constant for Pr=50. The minimum value of Nusselt number occurs at Pr=0.03. For W/D=2.5, figure (10), the minimum value of Nusselt number obtains at Pr=0.03, then the Nu increases by 2.5 at Pr=0.7. The Nusselt number slightly increases at Pr=7 and its value do not change for Pr=50. For W/D=5, figure (11), the Nusselt number increases with increasing the Prandtl number. The minimum Nusselt number value obtains at Pr=0.03, then the Nusselt number increases by a value of 2 at Pr=0.7. The Nusselt number increases slightly to reach maximum value at Pr=50.

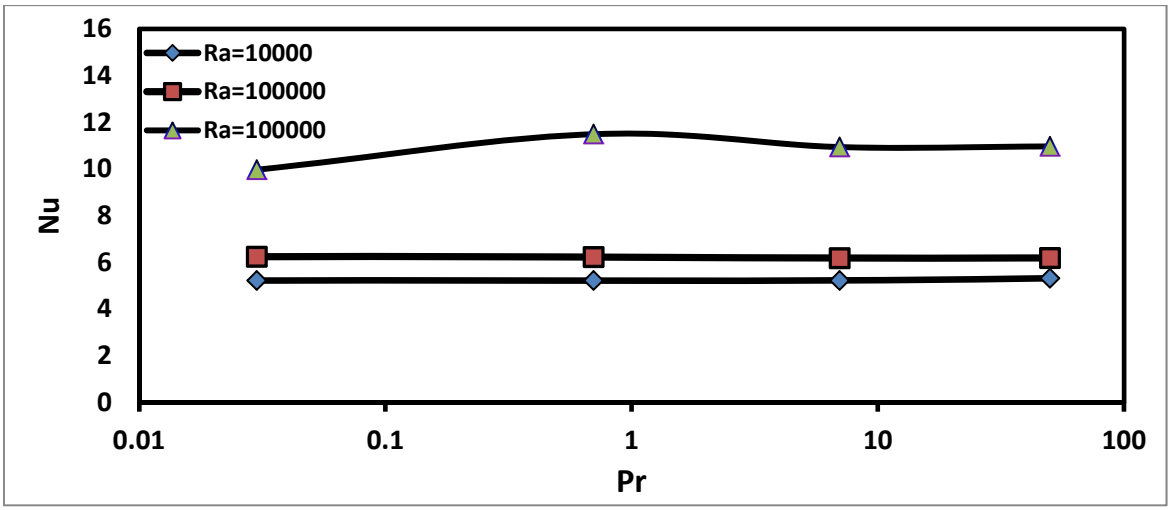

Figure (9) Effect of Prandtl number on the average Nusselt number for W/D=1.67.

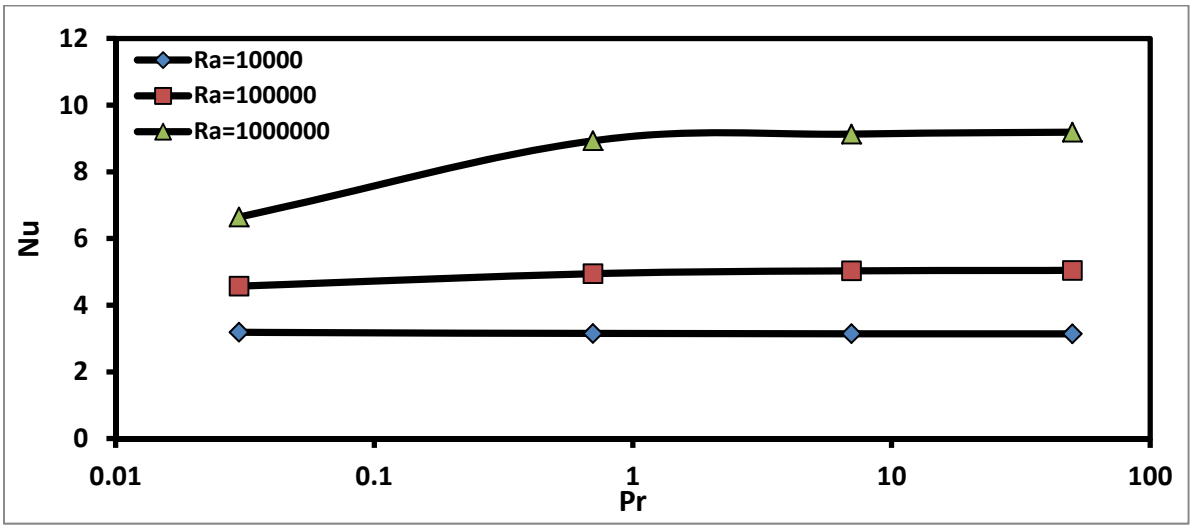

Figure (10) Effect of Prandtl number on the average Nusselt number for W/D=2.5.

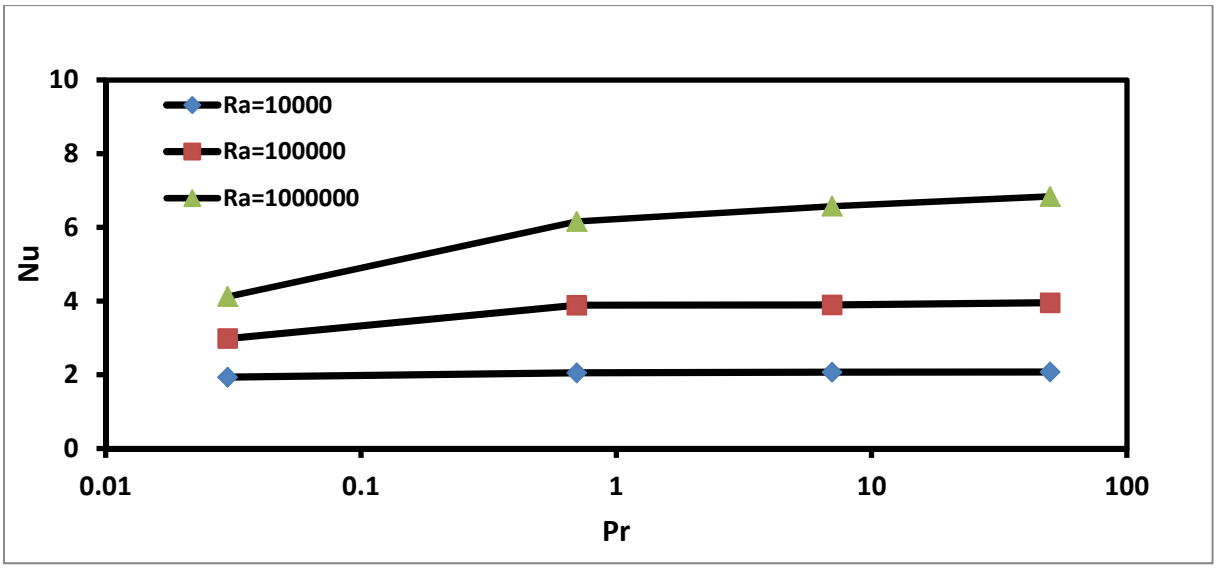

Figure (11) Effect of Prandtl number on the average Nusselt number for W/D=1.67.

CONCLUSIONS

Effect of Prandtl number on the natural convection heat transfer from circular horizontal cylinder in a square enclosure was investigated numerically over a fairly wide range of Ra with taking the effect of enclosure width. The main conclusions of the present work can be summarized as follows:

1. The numerical results show that the Nusselt number increases with increasing the Raylieh number for all cases.
2. The flow patterns and isotherms display the effect of Ra, enclosure width, and Prandtl number on the thermal and hydrodynamic characteristics.
3. The results show that the streamlines and isotherms for Pr=0.03 are unique and differ from those of other higher Prandtl numbers for all enclosure widths and $Ra \geq 10^5$.
4. The Conduction is the dominant of the heat transfer at $Ra=10^4$ for all Prandtl numbers. The contribution of the convective heat transfer increases with increasing the Raylieh number.
5. The streamlines and isotherms for $Pr \geq 0.7$ are nearly similar and independent of Prandtl number.
6. The results show that the Nusselt number for Pr=0.03 is unique and differ from those of other higher Prandtl numbers for all enclosure widths.
7. The enclosure width to the cylinder diameter has an influence on the results of the Nusselt number for Pr=0.03.

REFERENCES

Kuehn TH, Goldstein RJ., (1976). An experimental and theoretical study of natural convection in the annulus between horizontal concentric cylinders. Journal of Fluid Mechanics, Vol. 74, pp. 695–719.

Ekundayo CO, Probert SD, Newborough M, 1998. Heat transfer from a horizontal cylinder in a rectangular enclosure. Applied Energy, Vol. 61, pp. 57–78.

Moukalled F., Acharya S., (1996). Natural convection in the annulus between concentric horizontal circular and square cylinders. Journal of Thermophysics and Heat Transfer; Vol. 10(3), pp. 524 –531.

C. Shu; and Y. D. Zhu, (2002). Efficient computation of natural convection in a concentric annulus between an outer square cylinder and an inner circular cylinder. International Journal For Numerical Methods In Fluids, Vol. 38, pp. 429-445.

Koca, H.F. Oztop, Y. Varol, (2007). The effects of Prandtl number on natural convection in triangular enclosures with localized heating from below. Int. Commun. Heat Mass Transfer, Vol. 34, pp. 511–519.

Zi-Tao Yua, Ya-Cai Hua, Li-Wu Fanb, Ke-Fa Cenc, (2010). A Parametric Study of Prandtl Number Effects on Laminar Natural Convection Heat Transfer From a Horizontal Circular Cylinder to Its Coaxial Triangular Enclosure. Numerical Heat Transfer, Part A: Applications, Vol. 58, pp. 564–580.

Ali O. M. (2008), "Experimental and Numerical Investigation of Natural Convection Heat Transfer From Cylinders of Different Cross Section Cylinder In a Vented Enclosure," Ph. D., Thesis, College of Engineering, University of Mosul.

Bejan A. and Kraus A. D., (2003). Heat Transfer Handbook. John Wiley & Sons, Inc., Hoboken, New Jersey.

Thomas P. D., and Middlecoff J. F., 1980. Direct Control of the Grid Point Distribution in Meshes Generated by Elliptic Equations. AIAA Journal, Vol. 18, No. 6, pp. 652-656.

Hoffmann K. A., (1989). Computational Fluid Dynamics For Engineers. Engineering Education System, USA.

John D. Anderson Jr., (1995). Computational Fluid Dynamics, the Basics with Applications. McGraw–Hill Book Company.

Fletcher C.,A.,J., (1988). Computational Techniques for Fluid Dynamics 2. Springer, Verlag.

Petrović Z., and Stupar S., (1996). Computational Fluid Dynamics, One. University of Belgrade.

Thompson J. F., Warsi Z. U. A. and Mastin C. W., (1985). Numerical Grid Generation: Foundations and Applications. Mississippi State, Mississippi.

Roache, P., J., (1982). Computational Fluid Dynamics. Hermosa publishers.

Ferziger J. H. and Peric M., (2002). Computational Methods for Fluid Dynamics. Springer, New York.

پوختە

دڤی ڤەکولینی بخو فە گریدایە ب خواندنا تیوری بو ڤەکوهاستنا گەرماتیی ژ باراکی سەروشتی ل لولەك دەرژکەری بە شیوەکی بازنەیی ل کورەکی کەرتی. ئەف شولا دیاردەکیت تیستەکی ژ گرەنگیا گوهورینا ژماریت براندتل (0.03، 0.7، 7، و50)، ژماریت رایلی (10^4، 10^5، 10^6) وگوهورینا ریژیت ستیرادیت کورەکی بو تیرەی بازنە یا لولەکی W/D (1.67، 2.5، 5). شولی تیوری بیکتیت ژ شیکارکەرنا هاوکیشییت جیاکاریانە دادەریژیت فورتیسیق–ئیشییت جوگە وهاتە گهورین بو سیستەمی ریکیەخات ییت دەکونجیت بو لاشی. هاتە بکارئینان بو جارا ئیگی ریگە جەبری بو وەچە توڕی ژ بەر نواندنا ناوچە فیزیاوی نێوان لوولەکا ئاسوێی و کلوڕی داخراو . باشی هاتە دووبارە کردنەوە وەچە توڕی بریگە جیاکاریانە بەشی. هاتە بکارئینان ریگە جیاوازی دیاریکراو بو شیکارکەرنا سیستەمی هاوکیشییت جیاکاریانە.

بەراورد کردن ییت ئەنجامی ڤی ڤەکولینی دی گەل ڤەکولینییت تیوری ییت پیشوو، وهاتا دیارکرن کو ئەنجام ریکوتن نامە. پشکنین ل سەر گرنگیا کهورینا ژماریت براندتل ل سەر ژمارا نسلت، هێلّیت ریڕەو، وهێلّیت پلای گەرماتیی دەڤ ژمارییت رایلی جیاواز وریژییت ستیرادیت کورەکی بو تیرەی بازنە یا لولەکی جیاواز. ئەنجام پیشاندەدات کو هێلّیت ریڕەو، وهێلّیت پلای گەرماتیی دەڤ ژمارا براندتل 0.03 هەیە رەوشتەکی بێهاوتا وجیاوزیدەبێت ژ چونیەك دەڤ ژمارییت براندتل ییت مەزەن بو هەمی قەباریت ستیرادیت وبو ژمارییت رایلی مەزنتەر ژ 10^5. هێلّیت ریڕەو، وهێلّیت پلای گەرماتیی دەڤ ژمارییت براندتل یەکسان یان گەورە تەر ژ 0.7 نزیکەی چونیەك وسەربەخۆ ژ ژمارا براندتل. هەروەها دووبارەی دەکاتەوە هەمان رەوشتی بو ژمارا نسلت بو هەموو ژمارییت براندتل وبو هەموو ریژییت ستیرادیت کورەکی بو تیرەی بازنە یا لولەکی.

دراسة عددية لتأثيرات عدد براندتل على انتقال الحرارة بالحمل الطبيعي من اسطوانة دائرية داخل تجويف مغلق

الملخص

يتناول البحث الحالي دراسة عددية لانتقال الحرارة بالحمل الطبيعي من اسطوانة دائرية افقية موضوعة في تجويف مغلق. ويتضمن العمل فحص تأثير عدد براندتل على خصائص الجريان وانتقال الحرارة. يستخدم الدراسة اعداد براندتل مختلفة (0.03، 0.7، 7، و50)، اعداد رايلي مختلفة (10^4، 10^5، و10^6) ونسب مختلفة لعرض التجويف الى قطر الاسطوانة W/D (1.67، 2.5، و5). الحل العددي يتضمن حلا للمعادلات التفاضلية في صيغة الدوامية–دالة الجريان والمتحولة إلى نظام إحداثيات المطابقة للجسم. استخدمت الطريقة الجبرية للتوليد الشبكي بشكل مبدئي لتمثيل المنطقة الفيزيائية الواقعة بين الاسطوانة الأفقية الساخنة والحيز المغلق وتم إعادة التوليد الشبكي باستخدام الطريقة التفاضلية الجزئية. استخدم طريقة الفروق المحددة لحل نظام المعادلات التفاضلية.

تم مقارنة النتائج مع نتائج نظرية سابقة، واظهرت النتائج تطابقا جيدا. تم فحص تأثير اختلاف عدد براندتل على عدد نسلت، خطوط الجريان، وخطوط ثبوت درجات الحرارة عند اعداد رايلي مختلفة ونسب مختلفة لعرض التجويف الى قطر الاسطوانة. اظهرت النتائج ان خطوط الجريان وخطوط درجات الحرارة للحالة عند عدد براندتل مساوي الى 0.03 له تصرف منفرد ومختلف تماما عن مثيلاتها لأعداد براندتل عالية لمختلف الاحجام لعرض التجويف ولأعداد رايلي اكبر او يساوي 10^5. خطوط الجريان وخطوط درجات الحرارة لأعداد براندتل يساوي او اكبر من 0.7 متشابهة تقريبا ومستقلة عن عدد براندتل. ويتكرر نفس التصرف لعدد نسلت لأعداد براندتل المنخفضة والعالية مع كل النسب لعرض التجويف الى قطر الاسطوانة.